Cheminformatics Application in the Phytochemical and Biological Study of *Eucalyptus globulus* L. Bark as a Potential Hepatoprotective Drug

Khaled A. Nematallah,* Sahar Elmekkawy, Maha R. A. Abdollah, Mohey M. Elmazar, Essam Abdel-Sattar, and Meselhy Ragab Meselhy
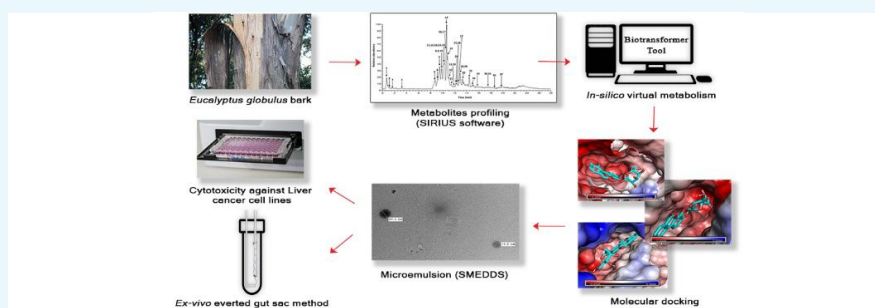
Read Online

ACCESS | Metrics & More | Article Recommendations | SI Supporting Information

"*E. globulus* bark photograph courtesy of 'Gwenvidig'. Copyright 2015"

ABSTRACT: Natural products are considered as a good source of antifibrotic agents, but identifying and isolating bioactive molecule(s) is still challenging. Fortunately, numerous computational techniques have evolved to save time and efforts in this field. The aim of the current study was to utilize several cheminformatics software to study the chemical and biological features of the bark of *Eucalyptus globulus* cultivated in Egypt. Sirius software, with the aid of online databases, was used to process liquid chromatography−mass spectrometry (LC−MS) chemical profiling and predict precise molecular formulae, chemical classes, and structures. Accordingly, 37 compounds were tentatively identified, including 15 reported here for the first time from this species. Also, the BioTransformer tool was successfully applied for in silico virtual study of the human metabolism of these compounds, and 1960 different products were obtained through various metabolic pathways. Finally, an electronic library of the identified compounds and their metabolites were developed and docked in silico against eight different protein targets that are involved in the liver fibrosis process. The results revealed that the extract may have a potential hepatoprotective effect through several mechanisms and that the metabolites have the highest binding affinities to the relevant enzymes than their parent compounds. The extract was found to show potent cytotoxic activity against the liver cancer cell lines HEPG2 and HUH-7, and its absorption was enhanced through nanoformulation, as proved using the ex vivo everted gut sac method.

1. INTRODUCTION

Eucalyptus globulus Labill. is an evergreen tree that belongs to the family Myrtaceae and is cultivated worldwide.[1] In Egypt, several *Eucalyptus* species are grown as line plantings and used for shade, construction timbers, and poles or fuelwood. In the Eucalyptus industry, the bark is considered as one of the main by products. Eucalyptus bark is considered as a good source of phenolic compounds with diverse biological activities.[2,3]

Polyphenols have several applications in cosmetics, food, and pharmaceutical industries. This class of compounds is known to demonstrate antioxidant, antimicrobial, antidiabetic, anti-inflammatory, antihyperlipidemic, hepatoprotective, nephroprotective, cardioprotective and, anticancer effects.[4] Ingestion of polyphenol-rich extracts such as green tea drink was found to be beneficial in reducing the risk of cancer incidence

and mortality.[5] However, its poor bioavailability, fast metabolism in the gastrointestinal tract (GIT) and the liver, and rapid elimination from the body hinder its utilization in the pharmaceutical industry.[6] Generally, the bioavailability of polyphenols could be enhanced by increasing their solubility and dissolution rate in the gastrointestinal fluid. Several techniques were used for improving solubility such as solid-

lipid nanoparticles, nanostructured lipid carriers, nanoemulsion, liposomes, and self-micro emulsifying drug-delivery systems (SMEDDS).[7]

Recently, several cheminformatics software have been developed to reduce time and cost in developing bioactive molecules. Several in silico tools for the prediction of absorption, distribution, metabolism, and toxicity were successively employed.[8] Furthermore, molecular docking studies were applied to predict the efficacy in terms of its binding to human target proteins and reduce efforts in in vitro and preclinical in vivo studies.

In the present study, the ethanolic extract of *E. globulus* cultivated in Egypt was chemically characterized by the spectrophotometric estimation of the total phenolics and flavonoid contents, profiling using ultrahigh-performance liquid chromatography−electrospray ionization−quadrupole time-of-flight tandem mass spectrometry (UPLC-ESI-QTOF-MS−MS) as well as its antioxidant activity. Consequently, the hepatoprotective effect of the extract was evaluated in light of recent cheminformatics software. In addition, the cytotoxic activities of the extract against two liver cancer cell lines (HEPG2 and HUH-7) were determined. SMEDDS was applied to enhance the intestinal absorption of the extract, which was assessed ex vivo using the everted gut sac method.

2. MATERIALS AND METHODS

2.1. General Experimental Procedures. Diaion HP-20, 2,2-diphenyl-1-picrylhydrazyl (DPPH), 2,2′-azino-bis (3-ethyl-benzothiazoline-6-sulfonic acid) (ABTS), 2,4,6-tris(2-pyridyl)-*s*-triazine (TPTZ), ascorbic acid, fluoresceine, ferrozine, aluminum chloride, and all other chemicals were purchased from Sigma-Aldrich, (Schnelldorf, Germany). Rutin and gallic acid were purchased from Sigma Chemical Co. (St. Louis, Mo, USA). The Folin−Ciocalteu reagent was from Loba-Chemie (Mumbai, India). Propylene glycol monocaprylate (Capryol 90) and diethylene glycol monoethyl ether (Transcutol P) were kindly supplied by Gattefossé (Saint Priest, France). LC−MS analysis was carried out on a Waters Acuity UPLC system, and all spectrophotometric analyses were conducted on microplate reader BMG Labtech FluoStar Omega (Ortenberg, Germany). All solvents used for extraction were of analytical grade, while solvents used for LC−MS analysis were of HPLC-mass grade.

2.2. Plant Material. The bark of *Eucalyptus globulus* L was collected in April 2019 from Medicinal, Aromatic and Poisonous plants Experimental Station, Faculty of Pharmacy, Cairo University, Giza, Egypt. The plant material was identified by Eng. Therease Labib, Consultant Taxonomist, Orman Botanic Garden, and a voucher specimen (No.16.8.2021) has been deposited in the herbarium of the Faculty of Pharmacy, Cairo University, Cairo, Egypt.

2.3. Extraction. One kilogram of powdered *E. globulus* L. bark was repeatedly extracted with 70% ethanol (3 × 5 L) by maceration till exhaustion. The combined filtrate was evaporated under reduced pressure to give 125 g of dry residue. Part of the residue (10 g) was loaded onto a column of Diaion HP-20 (50 cm length × 7 cm width) and eluted with water (3 L), followed by ethanol (3 L). The ethanol eluate was evaporated to dryness to give 7.2 g of ethanolic extract, which is rich in polyphenols (EE).

2.4. Chemical Characterization of the Extract. *2.4.1. Determinations of Total Phenol and Total Flavonoid Contents.* The Folin−Ciocalteu method using gallic acid as a standard was adopted to determine the total phenol content (TPC) of EE, as described before.[9] The measurement was performed at 630 nm (for TPC) and 420 nm (for TFC). Total phenols were expressed as gallic acid equivalents (GAE) mg/g extract (dw) using a calibration curve of a freshly prepared gallic acid solution. The total flavonoid content (TFC) was quantified using the aluminum chloride colorimetric method, as reported by Herald and Gadgil.[10] The TFC was expressed as rutin equivalents (RE) mg /g extract (dw).

2.4.2. UPLC-ESI-QTOF-MS−MS of EE of E. globulus Bark. High-resolution LC−MS−MS was carried out on an Acuity UPLC system (Waters) equipped with an HSS T3 column (100 × 1.0 mm, particle size 1.8 μm; Waters). The mobile phase was composed of two solvents: 0.1% formic acid in water (A), 99.9% acetonitrile, and 0.1% formic acid (B), at a flow rate of 150 μL/min. The binary gradient of the mobile phase was 0−1 min, 5% B; 1−16 min 5−95% B; 16−18 min, 95% B; 18−20, 5% B. EE was dissolved in 5% acetonitrile with a concentration of 1 mg/mL and then filtered using a syringe filter with a pore size 0.2 μm. The sample injection volume was 3.1 μL (full loop injection). Eluted compounds were detected from m/z 100 to 1000 with a resolution of 100,000 in the negative-ion mode using the following instrument settings: nebulizer gas, nitrogen, 1.6 bar; dry gas, nitrogen, 6 liters min^{-1}, 190 °C; capillary, −5500 V; in-source CID energy, 0 V; hexapole RF, 100 Vpp; quadrupole ion energy, 5 eV; collision gas, argon; collision energy, 10 eV; collision RF 200/400 Vpp (timing 50/50); transfer time, 70 μs; prepulse storage, 5 μs; pulser frequency, 10 kHz; spectra rate, 3 Hz. Internal mass calibration was performed by the infusion of 20 μL of 10 mM lithium formate in isopropanol: water, 1:1 (v/v), at a gradient time of 18 min using a diverter valve.

2.4.3. Tentative Identification of the Secondary Metabolites. The tentative identification of the metabolites of EE was carried out using Sirius software (ver. 4.7.4), which is available through https://bio.informatik.uni-jena.de/software/sirius/ as a free open-source software to predict the fragmentation and the molecular formulae.[11] The chemical structures were predicted by CSI: FingerID,[12] while CANOPUS was used for the prediction of natural product classes directly from MS/MS.[13]

2.4.4. Antioxidant Activities. 2.4.4.1. DPPH Assay. The DPPH assay method is based on the use and reduction of the free radical of DPPH.[14] The absorbance was measured at 517 nm in a microplate reader. The control and reference compound ascorbic acid were also measured. The experiment was carried out in triplicate, and the radical scavenging activity (Inhibition %) was calculated according to the following equation:

$$\%\text{inhibition} = [(A\text{ blank} - A\text{ sample})/A\text{ blank}] \times 100$$

The result was presented as IC$_{50}$ (μM).

2.4.4.2. ABTS Assay. The antioxidant capacity of sample to scavenge ABTS (2,2′-azino-bis(3-ethylbenzothiazoline-6-sulfonic acid)) free radicals was evaluated according to the methodology proposed by Faitanin and Gomes.[15] The absorbance was measured at 690 nm using a microplate reader (Tecan, USA). Data are represented as mean ± SD according to the following equation:

$$\%\text{Inhibition} = [(A\text{ blank} - A\text{ sample})/A\text{ blank}] \times 100$$

The result was presented as μM ascorbic acid equivalent per mg extract (μM AAE/mg extract) according to the following calibration curve equation:

$$y = 0.1226x + 1.936; \; R^2 = 0.9996$$

2.4.4.3. Ferric Reducing Antioxidant Power Assay. The method of ferric reducing antioxidant power (FRAP) is based upon the reduction of Fe^{3+} to Fe^{2+}, which is chelated with 2,4,6-tris (2-pyridyl)-*s*-triazine (TPTZ) to form the Fe^{2+}-TPTZ complex. The measurements were carried out according to the method reported by Justino and Miranda,[16] according to the following the calibration curve equation:

$$(y = 0.0009x - 0.0039; \; R^2 = 0.9996)$$

Result was presented as μM ascorbic acid equivalents (AAE)/mg extract.

2.4.4.4. Metal Chelation Assay. The metal chelation assay (MCA) was carried out according to the method of Santos and Alvarenga Brizola.[17] At the end of incubation time, the decrease in the produced color intensity was measured at 540 nm using the microplate reader (Tecan, USA). Data are represented as mean $\pm$ SD according to the following equation:

$$\%\text{Inhibition} = [(A\;\text{blank} - A\;\text{sample})/A\;\text{blank}] \times 100$$

Results of the extract tested were presented as μM ethylenediaminetetraacetic acid (EDTA) equivalent/mg extract with the calibration curve equation:

$$(y = 0.8640x + 4.4797; \; R^2 = 0.9951)$$

2.4.4.5. ORAC Assay. The oxygen radical absorbance activity (ORAC) assay was carried out according to the method of Liang, Cheng.[18] Fluorescence measurement (485 EX, 520 EM, nm) was continued for 2.5 h (85 cycles, each 90 s). The results of the samples are presented as μM TE/mg sample using the linear regression equation extracted from the following calibration curve (linear dose-inhibition curve of Trolox)

$$y = 32356.3x + 989769.9 \; (R^2 = 0.9957)$$

2.5. Virtual Human Metabolism Prediction. The human metabolism of the tentatively identified compounds was virtually predicted using the Biotransformer tool.[8] The metabolism prediction was carried out using the Superbio metabolic transformation option to cover biotransformation occurring both in human tissues as well as the gut microbiota. The Biotransformer tool is freely available on https://biotransformer.ca/

2.6. Molecular Docking. All the docking studies were carried out using protein–ligand complexes with crystal structures. Before the docking process, the protein structures were processed by AutoDockTools GUI of AutoDock 4.2 software.[19] All Autodock software are freely available on https://autodock.scripps.edu/resources/. The processing included adding hydrogen atoms, removing water molecules and the co-crystallized ligands from the protein–ligand complexes, and the regulation of the amide groups in the side chains of asparagine and glutamine to modify their connections with nearby residues and atoms. After that, the docking process was continued using AutoDock Vina.[20] The target human receptors selected in this study were the ligand-binding domains (LBDs) of ZAP-70, Kaep1, Angio-II-Type-1, Jak-2, FGFR1 kinase-1,

EGFR, TGFβR1, and VEGFR-2. All the LBDs were retrieved from the RCSB Protein Data Bank.

2.7. Preparation of SMEDDS. The SMEDDS were prepared according to the method that was modified by Nematallah et al.[21] Capryol 90 was the oily phase, while Tween 80 was the surfactant, and Transcutol P was the cosurfactant with a ratio 12.5:53.5:34, respectively. EE was dissolved in the oil/surfactant mixture with the aid of sonication at 25 °C for 5 min. Then, Transcutol P was added while swirling and stirring. The prepared SMEDDS was stored in tightly sealed glass vials at a temperature range of 2−8 °C until further use.

2.8. Characterization of the Microemulsion. SMEDDS were reconstituted with 4 times the volume of distilled water to form a microemulsion for characterization. The mean diameter of the droplet (droplet size) and the size distribution (polydispersity index; PDI) of the formed microemulsion were measured using the dynamic light scattering technique at a scattering angle of 173° on Zetasizer Nano ZS (Malvern Instruments, UK). The shape and size of the droplets were further characterized using Jeol transmission electron microscopy (TEM) (JEM-1230, Japan), a microemulsion drop was placed on a copper-coated grid, and a piece of filter paper was used to remove excess microemulsion. The magnification was 100,000× with an operating voltage of 80 kV.

2.9. Ex vivo Analysis of Microemulsion Absorption. The everted gut sac method was used to test the enhancement of the absorption of EE in intestines with the aid of microemulsion. The method was slightly modified from the method previously developed by Schilling and Mitra[22] and modified by Tambe and Mokashi.[23] The buffer used was a modified Kreb's Ringer phosphate bicarbonate (KRPB) solution, pH 7.4. Male Sprague−Dawley rats weighing 200−300 g were fasted for 16−20 h and anesthetized by an i.p. injection of 60 mg/kg pentobarbital. After making a midline incision in the abdomen, the small intestine was cut at two positions at 3 cm distal to the duodenum and at the ileocecal junction, carefully removed, and placed immediately in ice-cold saline solution. The intestines were segmented into 8−10 cm length segments, followed by eversion on a thin stainless-steel rod, rinsing with ice-cold saline solution, and then secured to the tip of a 1 mL disposable syringe barrel. The other end of the segment was ligated with silk thread and attached to the bottom of the everted gut sac set up. The everted gut sac was filled with a known volume (1−2 mL) of the modified KRPB buffer solution.

Each everted gut sac set up was filled with 25 mL of KRPB buffer. In one set up, a known amount of EE was suspended in the buffer, and the same amount of EE dissolved in the SMEDDS was added to the second setup. Each setup was left for 30 min at a temperature of 37 °C with simple agitation; then, the buffer inside the everted gut sac was withdrawn and tested for their content of extract spectrophotometrically.

2.10. Cytotoxicity Assay. Human hepatocellular (HCC) carcinoma cell lines (HEPG2 and HUH-7) were obtained from VACSERA (Giza, Egypt). The cells were maintained in Dulbecco's modified Eagle medium (DMEM) [+L-glutamine] supplemented with 10% fetal bovine serum, 100 units/mL of penicillin, 100 μg/mL of streptomycin, and 0.25 μg/mL amphotericin B (Gibco) at 37 °C in a humidified incubator containing 5% CO_2. All cell culture procedures were performed in a class II hood and incubations were done inside the incubator at 37 °C. Initial cytotoxicity screening of EE was investigated using the MTT (3-(4,5-dimethylthiazol-2-yl)-2,5-
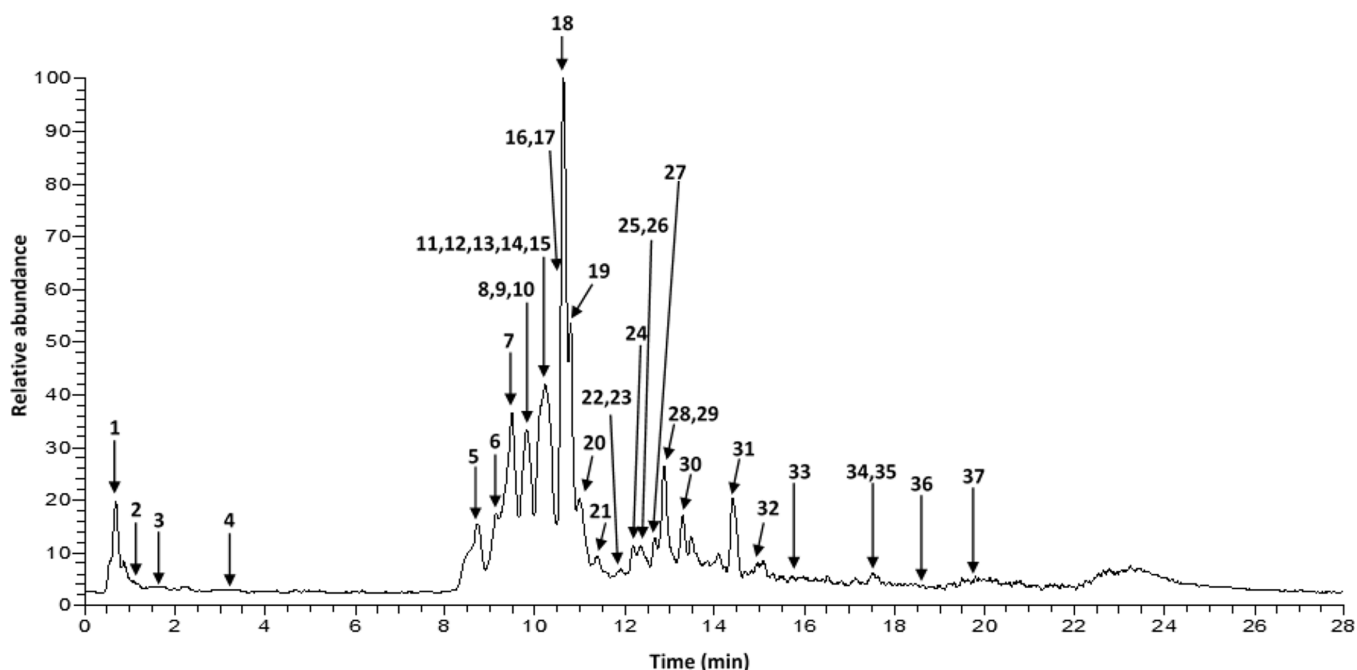
Figure 1. Total ion chromatogram of ethanolic *E. globulus* bark extract by UPLC-ESI-QTOF-MS−MS.

diphenyltetrazolium bromide) colorimetric cell viability assay that assess the cells' metabolic activity. Cells were seeded in 96-well plates at a density of 15,000 cells/well and allowed to attach overnight. Next day, the cells were treated with a serial dilution of EE at concentrations of 500, 250, 125, 62.5, 31.25, 15.625, 7.8, and 3.9 μg/mL for 72 h. Then, after 72 h, the culture medium was replaced with 100 μL/well of 5 mg/mL MTT powder solution dissolved in complete DMEM medium. Cells were then incubated for 2 h at 37 °C inside the incubator. Finally, the media was discarded, and the formed formazan crystals were dissolved in 100 μL/well DMSO and further incubated for 10 min at 37 °C inside the incubator. The optical density was then measured spectrophotometrically at 570 nm, and % cell viability was calculated relative to untreated controls. The inhibitory concentration 50 (IC_{50}) of the extracts on the different cell lines was determined via GraphPad Prism software (Ver 7.00, 2016, USA) using the nonlinear regression analysis.

3. RESULTS AND DISCUSSION

3.1. Extraction and Determination of Total Contents of Phenolics and Flavonoids.
In order to prepare an extract of *E. globulus* bark rich in phenolic compounds, the powdered bark was extracted with 70% ethanol and the extract was loaded onto a column of diaion-HP20. Elution started with water to remove salts, carbohydrates, or water-soluble impurities. Then, elution with ethanol yielded an extract rich in phenolics (EE). The total phenolics (TPC) and total flavonoid (TFC) contents of the EE were found to be 436.70 ± 34.63 μg GAE/mg extract and 7.32 ± 0.55 μg RE/mg extract, respectively. TPC of EE was found to be similar to that reported for the aqueous methanolic extract of *E. globulus* bark grown in Portugal,[24] and more than that reported in different types of extracts of *E. globulus* bark grown in Spain and Chile.[3,25]

3.2. UPLC-ESI-QTOF-MS−MS Analysis of the Extract.
For the first time, the extract of the bark of *E. globulus* growing in Egypt was analyzed using the high-resolution LC−MS−MS

technique in the negative-ion mode (Figure 1). Tentative identification of the metabolites was carried out on Sirius open-source software utilizing CSI: Finger ID and CANOPUS integrated tools.[11] Thirty-seven compounds were tentatively identified, including 12 phenolic acids derivatives, 4 flavonoids, 11 triterpene derivatives, and 5 fatty acids (Table 1).

Compounds **2, 3, 5, 7, 14, 15, 18, 24, 31, 33**, and **35−37** were detected before in the bark of *E. globulus*.[26−31] Compounds **10, 12, 21**, and **30** were detected for the first time in the barks of *E. globulus* cultivated in Egypt, but they were reported before in other organs like leaves and seedlings.[32−35] It is the first time for compounds **1, 13, 16, 22**, and **23** to be detected in this species, they were detected before in several *Eucalyptus* species like *E. grandis, E. urograndis, E. microcrys*, and *E. sideorxylon*.[36−38] Compounds **26, 27**, and **29** were detected here for the first time in genus *Eucalyptus*, but previously detected in other members of family Myrtaceae, *Myricaria floibunda, Psidium guajava*, and *Euginea florida*, respectively.[39−41] On the other hand, compounds **4, 9, 11, 17, 19, 20**, and **34** were detected for the first time in the family Myrtaceae.

3.3. Antioxidant Activity.
To evaluate the electron transfer and the hydrogen atom transfer capacity of the EE, DPPH, ABTS, FRAP, MCA, and ORAC tests were followed. Great diversity in the antioxidant activity of the EE was observed (Table 2). The extract showed high DPPH radical scavenging activity [IC_{50} value of 6.00 ± 0.21 μg/mL; relative to that of ascorbic acid used as standard (IC_{50} value of 28.87 ± 1.2 μg/mL)], and high ability to quench the $ABTS^+$ free radical (3054.1261 ± 131.69 μM AAE/mg extract). The FRAP activity of the EE was demonstrated to be 1469.63 ± 20.64 μM AAE/mg extract. The MCA of the EE was monitored to evaluate its ability to inhibit the interactions between metals and lipids. The EE showed high iron-chelating activity (163.19 ± 12.64 μM EDTA/mg extract). In addition, a high oxygen radical absorbance capacity of the EE was determined as an IC_{50} value of 2705.65 ± 444.75 μM TE/mg extract. It is worth mentioning that the EE is rich in TPC, and there is a direct

Table 1. Compounds Tentatively Identified in the Extract of *E. globulus* Bark by UPLC-ESI-QTOF-MS−MS

#	compound	R_t	area %	M-H	Ms/Ms	error (ppm)	molecular formula	structure score by Sirius (%)
1	hexahydroxydiphenoylhexoside	0.87	5.03	481.06171	301, 275	2.5	$C_{20}H_{18}O_{14}$	69.79
2	gallic acid	1.08	0.09	169.01418	125	−0.8	$C_7H_6O_5$	77.34
3	bis [hexahydroxydiphenoyl] hexoside	1.64	0.43	783.06708	765,721,481,301,271	0.7	$C_{34}H_{24}O_{22}$	71.00
4	galloylsedoheptulose	3.34	0.27	361.07706	249,231	0.1	$C_{14}H_{18}O_{11}$	52.85
5	catechin	8.74	2.66	289.07141	245,205,179	−1.4	$C_{15}H_{14}O_6$	78.99
6	flavonoltrisaccharide derivative	9.16	3.68	869.24969	707,525,407,289	2.2	$C_{39}H_{50}O_{22}$	64.59
7	galloylbis [hexahydroxydiphenoyl] hexoside	9.50	7.41	935.07825	917,873,783,633,571	−5.0	$C_{41}H_{28}O_{26}$	75.21
8	flavan dimer deoxy hexoside	9.75	1.71	707.19684	581,525,407,289	4.0	$C_{36}H_{36}O_{15}$	63.50
9	ellagic acid glucuronide	9.82	1.8	477.03046	301	−1.1	$C_{20}H_{14}O_{14}$	61.27
10	ellagic acid hexoside	9.87	1.89	463.05109	301	−1.8	$C_{20}H_{16}O_{13}$	77.66
11	procyanidin derivative	10.01	tr	721.17645	595,449,433,287	−1.7	$C_{36}H_{34}O_{16}$	43.64
12	hydroxy coumarin	10.05	1.24	161.02448	133,101,73	−1.8	$C_9H_6O_3$	57.58
13	ellagic acid pentoside isomer	10.11	2.82	433.04062	301	−1.3	$C_{19}H_{14}O_{12}$	51.05
14	trimethoxy phenyl galloylhexoside	10.23	2.19	497.12933	482,341,313,183,169	2.1	$C_{22}H_{26}O_{13}$	79.88
15	ellagic acid	10.30	2.08	300.99854	257,229	0.5	$C_{14}H_6O_8$	76.92
16	astilbin	10.51	0.88	449.1084	303,287,285,151	2.6	$C_{21}H_{22}O_{11}$	81.20
17	galloyllyoniresinolxylopyranoside	10.54	0.58	703.2229	688,537,315	−2.3	$C_{34}H_{40}O_{16}$	64.66
18	aromadendrinrhamnoside (engeletin)	10.64	27.00	433.11356	287,269,259	−1.5	$C_{21}H_{22}O_{10}$	80.84
19	dihyxosyl oxy octanol	10.93	0.25	469.22849	423	−2.5	$C_{20}H_{38}O_{12}$	57.81
20	flavangalloylhexoside	11.03	2.3	585.12378	433,287,259	2.9	$C_{28}H_{26}O_{14}$	71.13
21	lignan (buddlenol)	11.28	0.06	643.23883	595,417,387	−0.1	$C_{33}H_{40}O_{13}$	57.44
22	hydroxy-O-acetylhydroshengmanol-O-xylopyranoside	11.39	0.31	695.39923	649,487	−1.3	$C_{37}H_{60}O_{12}$	68.80
23	trihydroxy octadecenoic acid	11.60	0.10	329.23273	311,293,229,211,171	0.4	$C_{18}H_{34}O_5$	76.57
24	asiatic acid/arjunolic acid	12.17	0.33	487.34210	443,423	−0.6	$C_{30}H_{48}O_5$	62.37
25	triterpenoidal saponin derivative 1	12.32	0.07	459.11100	415	−1.6	$C_{28}H_{44}O_5$	66.74
26	messagenic acid I	12.37	0.28	473.32635	429,411,391	−2.8	$C_{29}H_{46}O_5$	78.73
27	guavalanostenoic acid/cleistocalyxic acid	12.61	0.03	501.32086	457,439,395	0.9	$C_{30}H_{46}O_6$	76.49
28	triterpenoidalsaponinderivative 2	12.73	0.50	529.35242	469	3.3	$C_{32}H_{50}O_6$	74.97
29	platanic acid	12.88	3.19	457.33179	413	−1.2	$C_{29}H_{46}O_4$	77.74
30	maslinic acid/corosolic acid	13.27	1.5	471.34723	425,407,397	−2.1	$C_{30}H_{48}O_4$	83.25
31	oleanolic acid, betulinic, and/or ursolic acid	14.43	3.65	455.35196	423,317	−1.6	$C_{30}H_{48}O_3$	60.25
32	triterpenoidalsaponin derivative 3	14.96	0.54	453.33655	224,135	−0.8	$C_{30}H_{45}O_3$	53.08
33	acetyl derivative of compound 31	15.81	0.48	497.36261	437	1.3	$C_{32}H_{50}O_4$	73.20
34	fatty acid derivative	17.44	0.25	341.26889	313,269	−2.5	$C_{20}H_{38}O_4$	49.66
35	hydroxydocosanoic acid (hydroxy behenic acid)	17.62	0.24	355.32132	309	1.4	$C_{22}H_{44}O_3$	45.99
36	hydroxytricosanoic acid	18.52	0.22	369.33701	323	1.3	$C_{23}H_{46}O_3$	53.83
37	hydroxy tetracosanoic acid	19.54	0.70	383.353236	337	−1.8	$C_{24}H_{48}O_3$	46.98

Table 2. In Vitro Antioxidant Activity of the Extract of *E. globulus* Bark[a]

method	DPPH assay	ABTS assay	FRAP assay	metal chelation assay	ORAC assay
% inhibition	NA	20.66	NA	11.52	NA
IC_{50} (μg/mL)	6.00 ± 0.21	NA	NA	NA	NA
substitution in the calibration curve equation (μM)	NA	152.71	73.48	8.16	135.28
μM AAE/mg extract	NA	3054.13 ± 131.69	1469.63 ± 20.65	NA	NA
μM EDTA /mg extract	NA	NA	NA	163.19 ± 12.64	NA
μM TE/mg extract	NA	NA	NA	NA	2705.65 ± 444.75

[a]AAE; ascorbic acid equivalent, IC_{50}; 50% inhibitory concentration, TE; Trolox equivalent, NA; not applicable.

relation between antioxidant activity and TPC that was previously reported for extracts of other plants.[42] The promising results of the antioxidant activity and richness of the extract with polyphenolic compounds encouraged us to utilize this extract as a hepatoprotective drug as it is well known that the main mechanism of the action of polyphenols as hepatoprotective drugs is mediated by decreasing the oxidation stress level in the liver.[43,44]

3.4. Virtual Human Metabolism Prediction. One of the main objectives of the current study is to prepare a nanoformulation that has the ability to enhance the bioavailability of the *E. globulus* extract as a hepatoprotective/antifibrotic drug. There are two approaches of the nanoformulations: the first one is the nanoformulation that protects the active principles from the human metabolic degradation and deliver the active drug to its site of action,

Table 3. Parent Compounds and the Metabolites with the Highest Binding Scores against the Eight Protein Targets

	parent compound		metabolite		silybin B	cocrystallized ligand
protein	name	score	name	score	score	score
JAK-2	astilbin (16)	−9.2	urolithin glucuronide derivative	−9.8	−2.9	−9.7
ACE	hedeargenin (stereoisomer of 25)	−9.2	urolithin glucuronide derivative	−9.4	−7.9	−8.6
ZAP Kinase	ellagic acid hexoside (10)	−9.4	ellagic acid glucuronide	−10.0	−8.4	−11.3
TGFβR-1	astilbin	−10.4	taxifolin glucuronide and pedunculosumoside D glucuronide	−10.1	−10.6	−10.5
Kaep-1	catechin (stereoisomer of 5)	−6.9	urolithin derivative	−8.4	−7.2	−7.5
FGFR-1	epicatechin (stereoisomer of 5)	−8.4	5,7,3′-trihydroxyflavanone sulfate	−9.3	−0.5	−10.8
VEGFR2	astilbin	−8.2	urolithin glucuronide derivative	−8.4	−7.0	−11.1
EGFR	ellagic acid (13), ellagic acid hexoside (10)	−8.6	5,7,3′-trihydroxyflavanone glucuronide	−9.3	−7.8	−9.5

while the second approach is the nanoformulations that enhance the solubility and absorption of the drug, leaving it susceptible to metabolic activation after absorption. The decision is mainly based on the activity of the parent compounds versus their metabolic products.

First, all the tentatively identified compounds from the LC−MS analysis were searched in the literature for their reported stereoisomers that result in the preparation of an electronic library of 47 different parent compounds. Subsequently, a virtual in silico metabolism was carried out for all those parent compounds using the Biotransformer tool.[8] The metabolism covered all the pathways including gut microbiota, EC-based, phase I and phase II metabolism. The process yielded an electronic library of 3093 metabolic products, and the number decreased to 1960 different metabolic products after the removal of the similar compounds (see the Supporting Information for full electronic library (.mol file) of the compounds and their metabolic products).

To validate the output of the virtual metabolism process, some of the metabolic products were compared with the reported metabolism processes in the literature. For example, from the 39 reported metabolic products of epicatechin, 37 compounds were successfully predicted using the Biotransformer tool.[8] Similarly, all the reported urolithin derivatives and their glucuronide glycosides in a study that was carried out by Tomas−Barberan, Garcia−Villalba[45] were found to be predicted successfully.

3.5. Molecular Docking. Molecular docking studies were carried out to evaluate the liver antifibrotic ability of *E. globulus* bark extract. The studies included both the parent-identified compounds as well as their metabolic products. The multitargeted approach focusing on different pathways is the most promising therapeutic strategy against fibrotic diseases.[46] Totally, 2008 molecules were docked against eight human protein targets that are involved in the liver fibrosis process. The results demonstrated a promising binding ability (Table 3). Collectively, the metabolic products showed binding affinities higher than their parent compounds as one of the parent compounds showed the highest binding affinity to a single target, while the metabolites showed the highest affinity to the other seven targets.

3.5.1. Janus Kinase-2 Enzyme (JAK-2). JAK-2 in a nonreceptor tyrosine kinase enzyme, and it has the ability to activate the signal transducer and activator of transcription (STAT). In many studies, it is proved that JAK2/STAT3 signaling promotes fibrosis, angiogenesis, and inflammation in many diseases.[47] Therefore, targeting and inhibition of the JAK-2 enzyme may have a promising therapeutic for liver

fibrosis.[48] From the docking studies, it was found that the compound with the highest binding affinity with JAK-2 (PDB ID 3KCK) was a urolithin glucuronide derivative with a score of −9.8, forming five hydrogen bonds with GLU-898, MET-929, LEU-932, and ASP-994 (Figure 2A). This binding is nearly better than the binding of the cocrystallized ligand 3-chloro-4-(4H-3,4,7-triazadibenzo[cd,f]azulen-6-yl) (binding score −9.7) with only three hydrogen bond interactions with the active site on GLU-898, LEU-932, and PHE-995. The parent compound with the highest binding affinity was found to be the flavonoid astilbin (16) with score −9.2. This urolithin glucuronide derivative is a metabolic product that could be produced by several metabolic pathways from several phenolic products identified in the *E. globulus* extract such as hexahydroxy diphenoyl hexoside (1), bis [hexahydroxy diphenoyl] hexoside (3), galloyl bis [hexahydroxy diphenoyl] hexoside (7), ellagic acid glucuronide (9), ellagic acid hexoside (10), and ellagic acid (15), which comprise around 20% of the total UPLC chromatogram area, and the predicted bio-transformation pathway is illustrated in the Supporting Information (Figure S1).

3.5.2. Angiotensin II Receptor Type 1 (ACE). The renin−angiotensin system is frequently activated in patients with chronic liver diseases. Angiotensin II has been suggested to play an important role in liver fibrogenesis. It induces hepatic stellate cell proliferation and upregulates the transforming growth factor beta-1 expression.[48] Both a parent compound and a metabolic product showed much higher binding affinities when compared to the standard inhibitor drug olmesartan (score −8.6) and the control drug silybin B (score −7.9). The highest binding affinity with ACE (PDB ID 4ZUD) was for another urolithin glucuronide derivative (score −9.4), which is another metabolic product from the same mentioned parent compounds in JAK-2 (Figure S2). It forms seven hydrogen bonds with four amino-acid residues TYR-35, TYR-92, SER-105, and ARG-167, and it also has Pi-Pi interactions with residues TRP-84 and TYR-87 (Figure 2B).

3.5.3. Zeta-Chain-Associated Protein Kinase 70 (ZAP Kinase). One of the major signaling pathways that control the liver homeostasis, pathophysiology and regulation of the inflammation−fibrosis−cancer axis is nuclear factor-kappa B (NF-κB).[49] The ZAP kinase enzyme mediates the activation of NF-κB pathway through tyrosine phosphorylation. Thus, the inhibition of ZAP kinase could have a promising effect in the cessation of the liver fibrosis process by the indirect deactivation of NF-κB.[49] From the tested compounds, the compound with the highest binding affinity with ZAP kinase (PDB ID 1U59) is the metabolite ellagic acid glucuronide with
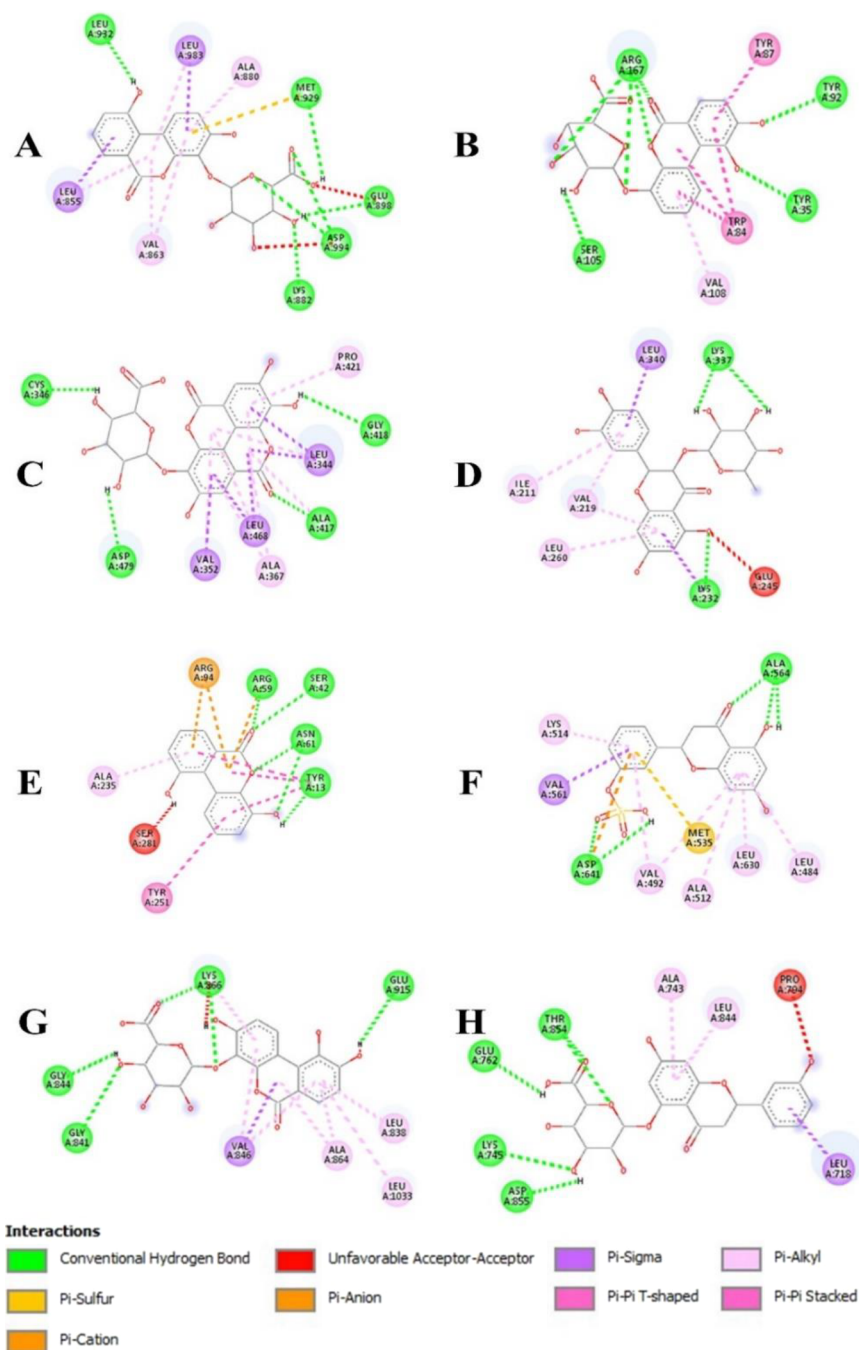
Figure 2. Ligand-binding domain of Janus kinase-2 and the urolithin glucuronide derivative (A). Ligand-binding domain of angiotensin II receptor type-1 and urolithin glucuronide derivative (B). Ligand-binding domain of zeta-chain-associated protein kinase-70 kinase and ellagic acid glucuronide (C). Ligand-binding domain of transforming growth factor beta receptor I and astilbin (D). Ligand-binding domain of Kelch-like ECH-associated protein-1 and urolithin derivative (E). Ligand-binding domain of fibroblast growth factor receptor-1 kinase and 5,7,3′-trihydroxyflavanone sulfate (F). Ligand-binding domain of vascular endothelial growth factor receptor-2 and urolithin glucuronide derivative (G). Ligand-binding domain of epidermal growth factor receptor and 5,7,3′-trihydroxyflavanone glucuronide (H).

score −10.0. Although the binding score of this metabolite is less than that of the cocrystallized ligand staurosporine (score −11.3), it forms a strong interaction with the active site through four hydrogen bonds with residues CYS-346, ALA-417, GLY-418, and ASP-479 (Figure 2C). This metabolite could be produced from the parent compounds ellagic acid (**15**), ellagic acid hexoside (**10**), and ellagic acid glucuronide (**9**) (Figure S3). Although there is an ellagic acid glucuronide (**9**) in the parent compounds, its binding score (−9.2) was less

than the metabolite, this could be due to different orientations of the glucuronide moiety in the active site.

3.5.4. Transforming Growth Factor Beta Receptor I (TGFβR-1). In most of the chronic liver diseases, the level of TGF-β increases markedly, activating the transformation of hepatic stellate cells to myofibroblasts and increased hepatocyte cell death, which causes liver fibrosis.[50] Therefore, the inhibition of TGF-β or blocking its downstream signaling pathway is one of the approaches to prevent liver fibrosis. The highest binding affinity with TGFβR-1 (PDB ID 2X7O) from
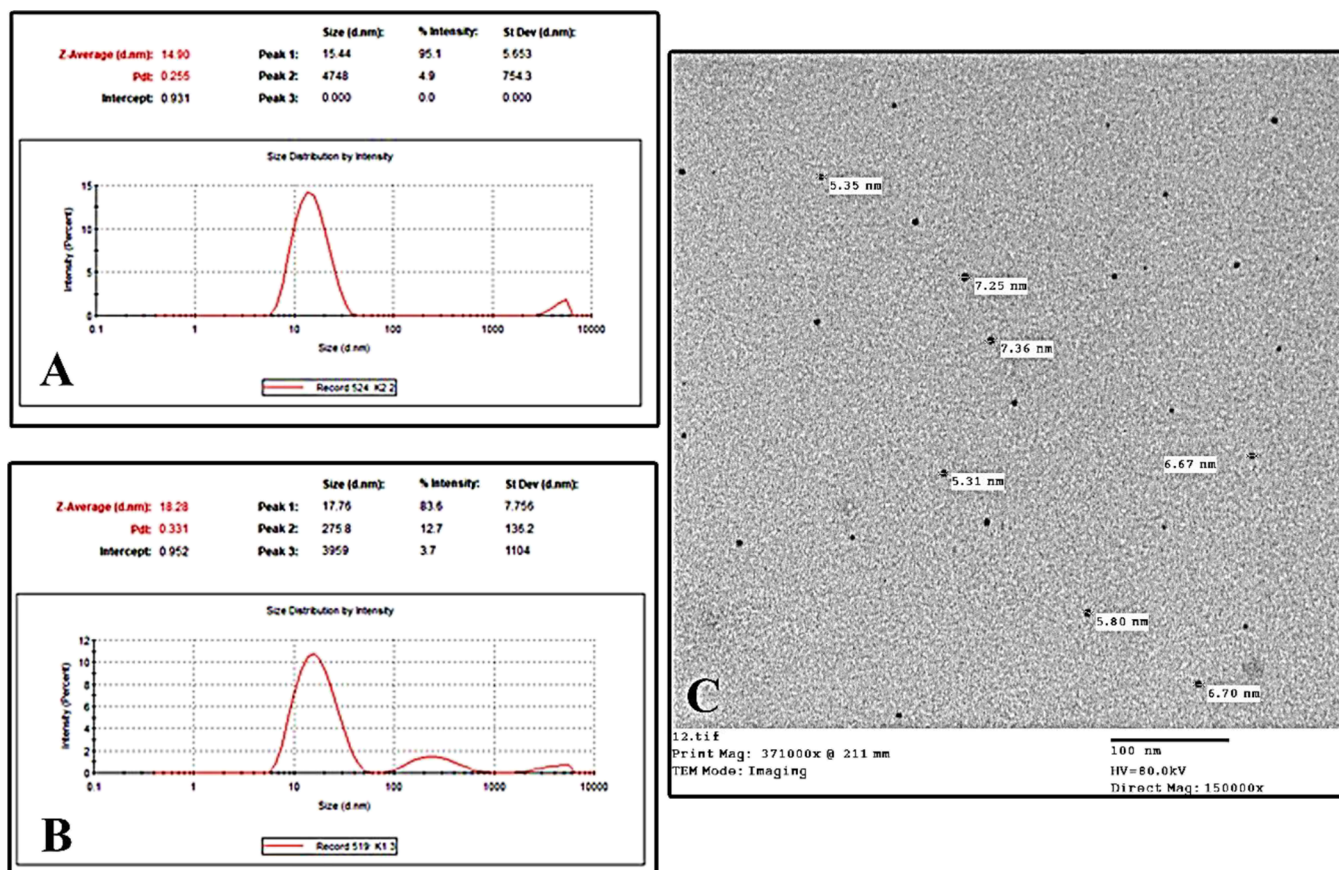
Figure 3. Characterization of the prepared microemulsion. (A) Droplet size using a zeta sizer of the microemulsion loaded with *E. globulus* extract; (B) droplet size using a zeta sizer of the void microemulsionl; (C) SEM illustration of the microemulsion droplets loaded with *E. globulus* extract (Mag. = 150,000×).

the tested compounds was found to be astilbin with a score of −10.4, which is the only parent compound that shows higher binding affinity than the metabolites against all the eight target proteins in the current study. There are also two flavonoid glycosides from the metabolites that showed a relatively promising binding affinity with the active site of TGFβR-1 with a score of −10.1. These results are promising when compared with the binding score of the cocrystallized ligand (3Z)-N-ethyl-N-methyl-2-oxo-3-[phenyl-[[4-(piperidin-1-ylmethyl)-phenyl]amino]methylidene]-1H-indole-6-carboxamide (−10.5). Astilbin forms three hydrogen bonds with residues LYS-232 and LYS-337. It also interacts by 4 pi-alkyl and 2 pi-sigma interactions with several amino-acid residues in the active site of TGFβR-1 (Figure 2D).

3.5.5. Kelch-Like ECH-Associated Protein 1 (Kaep1). Nrf2 protein is a key factor in the expression of the antioxidant defense system; phase II detoxifies enzymes by translocation into the nucleus and binding with the antioxidant responsive element.[51] Normally, Nrf2 is bound to Kaep1 protein, and it is activated by dissociation from Kaep1 by either Nrf2 phosphorylation or Kaep1 modification.[52] Finding a ligand with high binding affinity to Kaep1 will cause its modification and activation of Nrf2. Thus, targeting Kaep1 is considered beneficial, especially against liver diseases. One of the phenolic metabolites, which is a urolithin derivative, showed a very strong binding with Kaep1 (PDB ID 3VNG) with a score of −8.4 when compared with the binding score of the co-crystallized ligand 2-(3-((3-(5-(furan-2-yl)-1,3,4-oxadiazol-2-yl)ureido)methyl)phenoxy)acetic acid (−7.5). This metabolite

forms five hydrogen bonds with TYR-13, SER-42, ARG-59, and ASN-61 residues (Figure 2E). This metabolite is a result of metabolism of several parent phenolic compounds identified in *E. globulus* extract such as compounds **1, 3, 7, 9, 10**, and **15** (Figure S4).

3.5.6. Tyrosine Kinases. Tyrosine kinases (TKs) have a key role in the progression of liver fibrosis. TKs such as fibroblast growth factor receptor-1 (FGFR-1), vascular endothelial growth factor receptor 2 (VEGFR-2), and epidermal growth factor receptor (EGFR) have been reported as mediators for collagen synthesis and potential targets to antagonize liver fibrosis.[53,54] Targeting and blocking TKs have a potential inhibitory effect on hepatic stellate cells.[55] 5,7,3′-Trihydroxy-flavanone sulfate is a metabolite that is produced from the parent compound flavangalloyl hexoside (**20**) (Figure S5). It showed the highest binding affinity with both FGFR-1 with a score of −9.3. It forms with FGFR-1 (PDB ID 5B7V) five hydrogen bonds with the two amino-acid residues ALA-564 and ASP-641 (Figure 2F). These two residues also form hydrogen bonds with the cocrystallized ligand [5-amino-1-(2-methyl-1H-benzimidazol-6-yl)-1H-pyrazol-4-yl](1H-indol-2-yl)methanone. Another metabolite originating from the same parent compound no. **20**, which is 5,7,3′-trihydroxyflavanone glucuronide (Figure S7), has the highest binding score of −9.3 with EGFR (PDB ID 2J6M). It forms five hydrogen bonds with LYS-745, GLU-762, THR-854, and ASP-855 residues (Figure 2H). Regarding VEGFR2 (PDB ID 1YWN), the ligand with the highest binding affinity to its active site is a urolithin glucuronide derivative with a score of −8.4. It is a metabolic
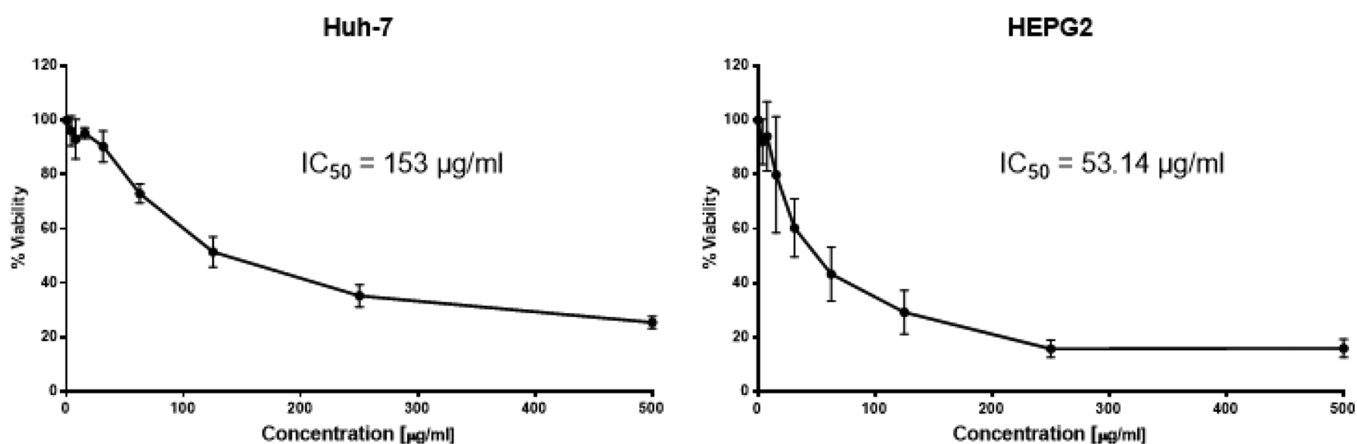
Figure 4. Effect of different concentrations of *Eucalyptus* bark extract on the percentage viability of hepatic carcinoma cell lines (HEPG2 and HUH-7) using the MTT cell viability assay after 72 h. Each point is the mean of six replicates, and error bars are for the standard deviation.

product from the phenolic compounds **1, 3, 7, 9, 10**, and **15** (Figure S6). It forms five hydrogen bonds with GLY-841, GLY-844, LYS-866, and GLU-915 residues (Figure 2G).

Collectively, it could be concluded from the docking studies that the metabolism products of the compounds identified in *E. globulus* extract are biologically active and have higher binding affinities to the protein targets under investigation in the current study. Furthermore, by the comparison of the binding affinities of these compounds with those of the cocrystallized ligand of each protein and silybin B as a reference hepatoprotective drug, it could be deduced that *E. globulus* bark extract has a promising liver antifibrotic activity and it could be included in further biological studies to prove its effect.

3.6. Preparation and Characterization of the Microemulsion. Based on the previous results of virtual metabolism and molecular docking, SMEDDS was chosen as an approach to enhance the bioavailability of EE. The EE was dissolved in a microemulsion system composed of Capryol 90, Tween 80, Transcutol P, and water. The size of the droplets loaded with *E. globulus* extract was measured using a zeta sizer and found to be 14.90 ± 1.2 nm with PDI 0.255 ± 0.032 (Figure 3A). Loading EE in the microemulsion has nearly no effect on the droplet size as the size of the void droplets was 18.28 ± 1.4 nm with PDI 0.331 ± 0.041 (Figure 3B). Additionally, the droplets were characterized by TEM, and it was found that the droplets have a spherical shape with uniform distribution with sizes ranging from 5 to 7 nm (Figure 3C).

In previous studies, nanoemulsions of *E. globulus* essential oil were prepared using grape seed oil and a hydrophilic surfactant to develop an efficient transdermal nanocarrier for the alternative analgesic therapy.[56] Also, urea formaldehyde nanocapsules loaded by a hydroalcoholic extract of *E. globulus* leaf extract were developed as a natural nanopesticide for pest control.[57]

To the best of our knowledge, the application of SMEDDS to enhance the bioavailability of *E. globulus* bark extract was reported here for the first time.

3.7. Ex Vivo Analysis of the Microemulsion Absorption. To study the effect of the microemulsion on the intestinal absorption of the EE, an everted gut sac technique was carried out. To determine the quantity of the EE, a collective UV−vis spectrophotometric calibration curve of EE dissolved in the microemulsion was established. The samples

were measured spectrophotometrically against a blank composed of void microemulsion at wavelength (λ_{max}) 278 nm. After 30 min of the experiment, only 9.5% of the extract suspended in water was transferred into the intestinal sac, while 24% of the extract dissolved in the microemulsion was absorbed successfully in the intestinal sac. This result indicates that SMEDDS enhanced the absorption of the *E. globulus* bark extract by nearly 2.5-fold.

The everted gut sac method is a known ex vivo technique to study the effect of several parameters on the absorption of drugs and its different formulations.[58] It was also used to study the absorption mechanisms of some herbal extracts such as *Schisandra chinensis* and *Inula cappa*.[59,60]

3.8. Cytotoxic Activity on Liver Carcinoma Cell Lines. MTT cytotoxicity assay results revealed that the EE possesses strong cytotoxic potential on two liver cancer cell lines (Figure 4). On the hepatic carcinoma cell lines, the extract was more potent on the HEPG2 cell line with IC$_{50}$ of 53.14 μg/mL compared to 153 μg/mL on HUH-7 cells.

Our results revealed a strong anticancer potential of the *E. globulus* bark extract on both tested cell lines with dose-dependent reduction in cell viability and calculated IC$_{50}$ of less than 300 μg/mL. The most potent effect was observed on HEPG2 cells, followed by HUH-7.

Even though the anticancer potential of *E. globulus* essential oils has been reported before, the potency of its bark extract on different cancer cell lines is still under investigation. *E. globulus* essential oil demonstrated the cytotoxic effect on colon cancer cell line SW48 and liver cancer cell line HepG2, normal human embryonic kidney cells HEK293t, and was toxic to the normal skin fibroblasts tested.[61] Another study by Teixeira et al. investigated the anticancer potential of the decoction extract of aerial leafy parts of *E. globulus* on colorectal (HCT-15), pancreatic (PANC-1), and nonsmall cell lung cancer (NCI-H460) cell lines with the highest potency observed on NCI-H460 cell lines. The cell cytotoxicity effect was attributed to the G0/G1 cell cycle arrest and an increase in the expression of tumor suppression proteins (e.g. p53, p21, and cyclin D1 proteins).[62] On the other hand, the bark extract of *E. globulus* was reported to cause a dose- and time-dependent reduction in the cell viability of MDA-MB-231 cell lines.[63] In line with the published reports, our findings further confirmed that *E. globulus* bark extract could be further developed for anticancer therapies.

4. CONCLUSIONS

The present findings clearly demonstrate that the integration of in silico-predicted biological activity profiles of the parent compounds and their metabolites was crucial in understanding the antifibrotic activity of the bark extract of *E. globulus* cultivated in Egypt. The bark extract was found to be a promising antifibrotic agent, and the predicted metabolites were more active than their parent compounds. Also, SMEDDS was effective in developing a more bioavailable formula with better metabolism and absorption. However, to the best of our knowledge, an investigation that combines the in silico estimates of drug metabolism and predictions of the biological activity profiles for both the parent drug and its metabolites has never been conducted. The results clearly demonstrate that the integration of in silico-predicted biological activity profiles of the parent drug substance and its metabolites improves the computer-aided assessments.

■ ASSOCIATED CONTENT

Ⓢ Supporting Information

The Supporting Information is available free of charge at https://pubs.acs.org/doi/10.1021/acsomega.1c07011.

> A full electronic library of the tentatively identified compounds of the ethanolic extract of *E. globulus* bark and their metabolic products after the removal of the repeated molecules (MOL)
> Virtual metabolic pathways of the compounds with the highest binding affinities to the protein targets under investigation (Figures S1−S7) (PDF)

■ AUTHOR INFORMATION

Corresponding Author

Khaled A. Nematallah − *Department of Pharmacognosy and Microbiology, Faculty of Pharmacy, The British University in Egypt (BUE), Cairo 11837, Egypt; The Center for Drug Research and Development (CDRD), Faculty of Pharmacy, BUE, Cairo 11837, Egypt;* ⓘ orcid.org/0000-0001-9550-6351; Phone: +2022689000 Ext. 1825; Email: khaled.nematallah@bue.edu.eg; Fax: +20226300010

Authors

Sahar Elmekkawy − *Department of Chemistry of Natural Compounds, National Research Centre, Giza 12622, Egypt;* ⓘ orcid.org/0000-0002-0826-6968

Maha R. A. Abdollah − *The Center for Drug Research and Development (CDRD), Faculty of Pharmacy, BUE, Cairo 11837, Egypt; Department of Pharmacology and Biochemistry, Faculty of Pharmacy, The British University in Egypt (BUE), Cairo 11837, Egypt*

Mohey M. Elmazar − *The Center for Drug Research and Development (CDRD), Faculty of Pharmacy, BUE, Cairo 11837, Egypt; Department of Pharmacology and Biochemistry, Faculty of Pharmacy, The British University in Egypt (BUE), Cairo 11837, Egypt*

Essam Abdel-Sattar − *Pharmacognosy Department, Faculty of Pharmacy, Cairo University, Cairo 11562, Egypt;* ⓘ orcid.org/0000-0002-5864-1674

Meselhy Ragab Meselhy − *Pharmacognosy Department, Faculty of Pharmacy, Cairo University, Cairo 11562, Egypt*

Complete contact information is available at:
https://pubs.acs.org/10.1021/acsomega.1c07011

Notes

The authors declare no competing financial interest.

■ REFERENCES

(1) Hayat, U.; Jilani, M. I.; Rehman, R.; Nadeem, F. A Review on *Eucalyptus globulus*: A New Perspective in Therapeutics. *Int. J. Chem. Biol. Sci.* **2015**, *8*, 85−91.

(2) Mota, M. I. F. D.; Pinto, P. C. O. R.; Novo, C. C.; Sousa, G. D. A.; Guerreiro, O. R. F. D. N.; Guerra, Â. D. C. R.; Duarte, M. F. P.; Rodrigues, A. E. *Eucalyptus globulus* bark as A source of polyphenolic compounds with biological activity. *O Papel* **2013**, *74*, 57−64.

(3) Vázquez, G.; Fontenla, E.; Santos, J.; Freire, M. S.; González-Álvarez, J.; Antorrena, G. Antioxidant activity and phenolic content of chestnut (*Castanea sativa*) shell and eucalyptus (*Eucalyptus globulus*) bark extracts. *Ind. Crops Prod.* **2008**, *28*, 279−285.

(4) Romano, B.; Pagano, E.; Montanaro, V.; Fortunato, A. L.; Milic, N.; Borrelli, F. Novel insights into the pharmacology of flavonoids. *Phytother. Res.* **2013**, *27*, 1588−1596.

(5) Cochrane Gynaecological, Neuro-oncology and Orphan Cancer Group; Filippini, T.; Malavolti, M.; Borrelli, F.; Izzo, A. A.; Fairweather-Tait, S. J.; Horneber, M.; Vinceti, M. Green tea (*Camellia sinensis*) for the prevention of cancer. *Cochrane Database Syst. Rev.* **2009**, *2009*, No. CD005004.

(6) D'Archivio, M.; Filesi, C.; Varì, R.; Scazzocchio, B.; Masella, R. Bioavailability of the polyphenols: status and controversies. *Int. J. Mol. Sci.* **2010**, *11*, 1321−1342.

(7) Bilia, A. R.; Isacchi, B.; Righeschi, C.; Guccione, C.; Bergonzi, M. C. Flavonoids Loaded in Nanocarriers: An Opportunity to Increase Oral Bioavailability and Bioefficacy. *Food Nutr. Sci.* **2014**, *05*, 1212−1327.

(8) Djoumbou-Feunang, Y.; Fiamoncini, J.; Gil-de-la-Fuente, A.; Greiner, R.; Manach, C.; Wishart, D. S. BioTransformer: a comprehensive computational tool for small molecule metabolism prediction and metabolite identification. *Aust. J. Chem.* **2019**, *11*, 2.

(9) Attard, E. A rapid microtitre plate Folin-Ciocalteu method for the assessment of polyphenols. *Open Life Sci.* **2013**, *8*, 48−53.

(10) Herald, T. J.; Gadgil, P.; Tilley, M. High-throughput micro plate assays for screening flavonoid content and DPPH-scavenging activity in sorghum bran and flour. *J. Sci. Food Agric.* **2012**, *92*, 2326−2331.

(11) Dührkop, K.; Fleischauer, M.; Ludwig, M.; Aksenov, A. A.; Melnik, A. V.; Meusel, M.; Dorrestein, P. C.; Rousu, J.; Böcker, S. SIRIUS 4: a rapid tool for turning tandem mass spectra into metabolite structure information. *Nat. Methods* **2019**, *16*, 299−302.

(12) Dührkop, K.; Shen, H.; Meusel, M.; Rousu, J.; Böcker, S. Searching molecular structure databases with tandem mass spectra using CSI:FingerID. *Proc. Natl. Acad. Sci. U. S. A.* **2015**, *112*, 12580−12585.

(13) Dührkop, K.; Nothias, L. F.; Fleischauer, M.; Reher, R.; Ludwig, M.; Hoffmann, M. A.; Petras, D.; Gerwick, W. H.; Rousu, J.; Dorrestein, P. C.; Böcker, S. Systematic classification of unknown metabolites using high-resolution fragmentation mass spectra. *Nat. Biotechnol.* **2021**, *39*, 462−471.

(14) Gutiérrez-Grijalva, E. P.; Antunes-Ricardo, M.; Acosta-Estrada, B. A.; Gutiérrez-Uribe, J. A.; Basilio Heredia, J. Cellular antioxidant activity and in vitro inhibition of alpha-glucosidase, alpha-amylase and pancreatic lipase of oregano polyphenols under simulated gastro-intestinal digestion. *Food Res. Int.* **2019**, *116*, 676−686.

(15) Faitanin, R. D.; Gomes, J. V. D.; Rodrigues, P. M.; Menezes, L. F. T. D.; Neto, Á. C.; Gonçalves, R. C. R.; Kitagawa, R. R.; Silveira, D.; Jamal, C. M. Chemical study and evaluation of antioxidant activity and a-glucosidase inhibition of *Myrciaria strigipes* O. Berg (Myrtaceae). *J. Appl. Pharm. Sci.* **2018**, *8*, 120−125.

(16) Justino, A. B.; Miranda, N. C.; Franco, R. R.; Martins, M. M.; Silva, N. M. D.; Espindola, F. S. Annona muricata Linn. leaf as a source of antioxidant compounds with in vitro antidiabetic and inhibitory potential against α-amylase, α-glucosidase, lipase, non-enzymatic glycation and lipid peroxidation. *Biomed. Pharmacother.* **2018**, *100*, 83−92.

(17) Santos, J. S.; Alvarenga Brizola, V. R.; Granato, D. High-throughput assay comparison and standardization for metal chelating capacity screening: A proposal and application. *Food Chem.* 2017, *214*, 515−522.

(18) Liang, Z.; Cheng, L.; Zhong, G. Y.; Liu, R. H. Antioxidant and antiproliferative activities of twenty-four *Vitis vinifera* grapes. *PLoS One* 2014, *9*, No. e105146.

(19) Morris, G. M.; Huey, R.; Lindstrom, W.; Sanner, M. F.; Belew, R. K.; Goodsell, D. S.; Olson, A. J. AutoDock4 and AutoDockTools4: Automated docking with selective receptor flexibility. *J. Comput. Chem.* 2009, *30*, 2785−2791.

(20) Trott, O.; Olson, A. J. AutoDock Vina: improving the speed and accuracy of docking with a new scoring function, efficient optimization and multithreading. *J. Comput. Chem.* 2010, *31*, 455−461.

(21) Nematallah, K. A.; Ayoub, N. A.; Abdelsattar, E.; Meselhy, M. R.; Elmazar, M. M.; El-Khatib, A. H.; Linscheid, M. W.; Hathout, R. M.; Godugu, K.; Adel, A.; et al. Polyphenols LC-MS2 profile of Ajwa date fruit (*Phoenix dactylifera* L.) and their microemulsion: Potential impact on hepatic fibrosis. *J. Funct. Foods* 2018, *49*, 401−411.

(22) Schilling, R. J.; Mitra, A. K. Intestinal mucosal transport of insulin. *Int. J. Pharm.* 1990, *62*, 53−64.

(23) Tambe, A.; Mokashi, P.; Pandita, N. *Ex-vivo* intestinal absorption study of boswellic acid, cyclodextrin complexes and poloxamer solid dispersions using everted gut sac technique. *J. Pharm. Biomed. Anal.* 2019, *167*, 66−73.

(24) Santos, S. A. O.; Villaverde, J. J.; Silva, C. M.; Neto, C. P.; Silvestre, A. J. D. Supercritical fluid extraction of phenolic compounds from *Eucalyptus globulus* Labill bark. *J. Supercrit. Fluids* 2012, *71*, 71−79.

(25) González, N.; Elissetche, J.; Pereira, M.; Fernández, K. Extraction of polyphenols: Experimental kinetics, modeling and evaluation of their antioxidant and antifungical activities. *Ind. Crops Prod.* 2017, *109*, 737−745.

(26) Santos, S. A.; Freire, C. S.; Domingues, M. R.; Silvestre, A. J.; Neto, C. P. Characterization of phenolic components in polar extracts of *Eucalyptus globulus* Labill. bark by high-performance liquid chromatography-mass spectrometry. *J. Agric. Food Chem.* 2011, *59*, 9386−9393.

(27) Yun, B.-S.; Lee, I.-K.; Kim, J.-P.; Chung, S.-H.; Shim, G.-S.; Yoo, I.-D. Lipid Peroxidation Inhibitory Activity of Some Constituents Isolated from the Stem Bark of *Eucalyptus globulus*. *Arch. Pharmacal Res.* 2000, *23*, 147−150.

(28) Gominho, J.; Lourenço, A.; Marques, A. V.; Pereira, H. An extensive study on the chemical diversity of lipophilic extractives from *Eucalyptus globulus* wood. *Phytochemistry* 2020, *180*, No. 112520.

(29) de Melo, M. M. R.; Oliveira, E. L. G.; Silvestre, A. J. D.; Silva, C. M. Supercritical fluid extraction of triterpenic acids from *Eucalyptus globulus* bark. *J. Supercrit. Fluids* 2012, *70*, 137−145.

(30) Parreira, P.; Soares, B. I. G.; Freire, C. S. R.; Silvestre, A. J. D.; Reis, C. A.; Martins, M. C. L.; Duarte, M. F. *Eucalyptus spp*. outer bark extracts inhibit *Helicobacter pylori* growth: *in vitro* studies. *Ind. Crops Prod.* 2017, *105*, 207−214.

(31) Freire, C. S. R.; Silvestre, A. J. D.; Neto, C. P. Identification of New Hydroxy Fatty Acids and Ferulic Acid Esters in the Wood of *Eucalyptus globulus*. *Holzforschung* 2002, *56*, 143−149.

(32) Boulekbache-Makhlouf, L.; Meudec, E.; Mazauric, J. P.; Madani, K.; Cheynier, V. Qualitative and semi-quantitative analysis of phenolics in *Eucalyptus globulus* leaves by high-performance liquid chromatography coupled with diode array detection and electrospray ionisation mass spectrometry. *Phytochem. Anal.* 2013, *24*, 162−170.

(33) Movsumov, I. S.; Aliev, A. M. Triterpenoid acids from some *Eucalyptus* specimens. *Khim. Prir. Soedin.* 1985, *2*, 271−272.

(34) Séro, L.; Sanguinet, L.; Blanchard, P.; Dang, B. T.; Morel, S.; Richomme, P.; Séraphin, D.; Derbré, S. Tuning a 96-well microtiter plate fluorescence-based assay to identify AGE inhibitors in crude plant extracts. *Molecules* 2013, *18*, 14320−14339.

(35) Araújo, P.; Ferreira, M. S.; de Oliveira, D. N.; Pereira, L.; Sawaya, A. C.; Catharino, R. R.; Mazzafera, P. Mass spectrometry

imaging: an expeditious and powerful technique for fast in situ lignin assessment in Eucalyptus. *Anal. Chem.* 2014, *86*, 3415−3419.

(36) Santos, S. A.; Vilela, C.; Freire, C. S.; Neto, C. P.; Silvestre, A. J. Ultra-high performance liquid chromatography coupled to mass spectrometry applied to the identification of valuable phenolic compounds from Eucalyptus wood. *J. Chromatogr. B Analyt. Technol. Biomed. Life Sci.* 2013, *938*, 65−74.

(37) Fortes, G. A. C.; Silva, A. J. R. D.; Ferri, P. H.; Santos, S. C. Phenolic Compounds from the Leaves of *Eucalyptus microcorys* F. Muell. *Rec. Nat. Prod.* 2015, *9*, 292−296.

(38) Okba, M. M.; El Gedaily, R. A.; Ashour, R. M. UPLC-PDA-ESI-qTOF-MS profiling and potent anti-HSV-II activity of *Eucalyptus sideroxylon* leaves. *J. Chromatogr. B Analyt. Technol. Biomed. Life Sci.* 2017, *1068-1069*, 335−342.

(39) Santos, P.; Gomes, L.; Mazzei, J.; Fontão, A. P.; Sampaio, A.; Siani, A.; Valente, L. Polyphenol and Triterpenoid Constituents of *Eugenia Florida* Dc. (Myrtaceae) Leaves and Their Antioxidant and Cytotoxic Potential. *Quim. Nova* 2018, *41*, 1140.

(40) de Azevedo, M. M. L.; Cascaes, M. M.; Guilhon, G.; Andrade, E. H. A.; Zoghbi, M.; da Silva, J. K. R.; Santos, L. S.; da Silva, S. H. M. Lupane triterpenoids, antioxidant potential and antimicrobial activity of *Myrciaria floribunda* (H. West ex Willd.) O. Berg. *Nat. Prod. Res.* 2019, *33*, 506−515.

(41) Bagri, P.; Ali, M.; Aeri, V.; Bhowmik, M. Isolation and antidiabetic activity of new lanostenoids from the leaves of *Psidium guajava* l. *Int. J. Pharm. Pharm. Sci.* 2016, *8*, 14−18.

(42) de Mello Andrade, J. M.; Fasolo, D. Polyphenol Antioxidants from Natural Sources and Contribution to Health Promotion. In *Polyphenols in Human Health and Disease*; Academic Press, 2014, pp. 253−265.

(43) Saha, P.; Talukdar, A. D.; Nath, R.; Sarker, S. D.; Nahar, L.; Sahu, J.; Choudhury, M. D. Role of Natural Phenolics in Hepatoprotection: A Mechanistic Review and Analysis of Regulatory Network of Associated Genes. *Front. Pharmacol.* 2019, *10*, 509.

(44) Ugwu, C. E.; Suru, S. M. Medicinal plants with hepatoprotective potentials against carbon tetrachloride-induced toxicity: a review. *Egypt. Liver J.* 2021, *11*, 88.

(45) Tomás-Barberán, F. A.; García-Villalba, R.; González-Sarrías, A.; Selma, M. V.; Espín, J. C. Ellagic acid metabolism by human gut microbiota: consistent observation of three urolithin phenotypes in intervention trials, independent of food source, age, and health status. *J. Agric. Food Chem.* 2014, *62*, 6535−6538.

(46) Rosenbloom, J.; Mendoza, F. A.; Jimenez, S. A. Strategies for anti-fibrotic therapies. *Biochem. Biophys. Acta* 2013, *1832*, 1088−1103.

(47) Zhao, J.; Qi, Y. F.; Yu, Y. R. STAT3: A key regulator in liver fibrosis. *Ann. Hepatol.* 2021, *21*, 100224.

(48) Granzow, M.; Schierwagen, R.; Klein, S.; Kowallick, B.; Huss, S.; Linhart, M.; Mazar, I. G.; Görtzen, J.; Vogt, A.; Schildberg, F. A.; Gonzalez-Carmona, M. A.; Wojtalla, A.; Krämer, B.; Nattermann, J.; Siegmund, S. V.; Werner, N.; Fürst, D. O.; Laleman, W.; Knolle, P.; Shah, V. H.; Sauerbruch, T.; Trebicka, J. Angiotensin-II type 1 receptor-mediated Janus kinase 2 activation induces liver fibrosis. *Hepatology* 2014, *60*, 334−348.

(49) Sun, B.; Karin, M. NF-kappaB signaling, liver disease and hepatoprotective agents. *Oncogene* 2008, *27*, 6228−6244.

(50) Fabregat, I.; Moreno-Càceres, J.; Sánchez, A.; Dooley, S.; Dewidar, B.; Giannelli, G.; ten Dijke, P.; the IT-LIVER Consortium. TGF-beta signalling and liver disease. *FEBS J.* 2016, *283*, 2219−2232.

(51) Chen, B.; Lu, Y.; Chen, Y.; Cheng, J. The role of Nrf2 in oxidative stress-induced endothelial injuries. *J. Endocrinol.* 2015, *225*, R83−R99.

(52) Lu, B.; Sun, T.; Li, W.; Sun, X.; Yao, X.; Sun, X. Piceatannol protects ARPE-19 cells against vitamin A dimer-mediated photo-oxidative damage through activation of Nrf2/NQO1 signalling. *J. Funct. Foods* 2016, *26*, 739−749.

(53) Yoshiji, H.; Kuriyama, S.; Yoshii, J.; Ikenaka, Y.; Noguchi, R.; Hicklin, D. J.; Wu, Y.; Yanase, K.; Namisaki, T.; Yamazaki, M.; et al. Vascular endothelial growth factor and receptor interaction is a

prerequisite for murine hepatic fibrogenesis. *Gut* **2003**, *52*, 1347−1354.

(54) Fuchs, B. C.; Hoshida, Y.; Fujii, T.; Wei, L.; Yamada, S.; Lauwers, G. Y.; McGinn, C. M.; DePeralta, D. K.; Chen, X.; Kuroda, T.; et al. Epidermal growth factor receptor inhibition attenuates liver fibrosis and development of hepatocellular carcinoma. *Hepatology* **2014**, *59*, 1577−1590.

(55) Qu, K.; Huang, Z.; Lin, T.; Liu, S.; Chang, H.; Yan, Z.; Zhang, H.; Liu, C. New Insight into the Anti-liver Fibrosis Effect of Multitargeted Tyrosine Kinase Inhibitors: From Molecular Target to Clinical Trials. *Front. Pharmacol.* **2016**, *6*, 300.

(56) Aziz, Z. A. A.; Nasir, H. M.; Ahmad, A.; Setapar, S. H. M.; Ahmad, H.; Noor, M. H. M.; Rafatullah, M.; Khatoon, A.; Kausar, M. A.; Ahmad, I.; et al. Enrichment of Eucalyptus oil nanoemulsion by micellar nanotechnology: transdermal analgesic activity using hot plate test in rats' assay. *Sci. Rep.* **2019**, *9*, 13678.

(57) Khoshraftar, Z.; Safekordi, A. A.; Shamel, A.; Zaefizadeh, M. Synthesis of natural nanopesticides with the origin of *Eucalyptus globulus* extract for pest control. *Green Chem. Lett. Rev.* **2019**, *12*, 286−298.

(58) Alam, M. A.; Al-Jenoobi, F. I.; Al-Mohizea, A. M. Everted gut sac model as a tool in pharmaceutical research: limitations and applications. *J. Pharm. Pharmacol.* **2012**, *64*, 326−336.

(59) Yang, J.-M.; IP, S. P. P.; J. Yeung, H. K.; Che, C.-T. HPLC-MS analysis of *Schisandra lignans* and their metabolites in Caco-2 cell monolayer and rat everted gut sac models and in rat plasma. *Acta Pharm. Sin. B* **2011**, *1*, 46−55.

(60) Gong, Z. P.; Li, M.; Hou, J. Y.; Wu, L. L.; Chen, T. T.; Li, Y. T.; Chen, S. Y.; Li, Y. J.; Wang, A. M.; Lan, Y. Y.; Wang, Y. L. Absorption of Inula cappa extract based on everted intestinal sac method. *Zhongguo Zhong Yao Za Zhi* **2018**, *43*, 609−617.

(61) Khazraei, H.; Shamsdin, S. A.; Zamani, M. In Vitro Cytotoxicity and Apoptotic Assay of *Eucalyptus globulus* Essential Oil in Colon and Liver Cancer Cell Lines. *J. Gastrointest. Cancer* **2021**, 1−7.

(62) Teixeira, A.; DaCunha, D. C.; Barros, L.; Caires, H. R.; Xavier, C. P.; Ferreira, I. C.; Vasconcelos, M. H. *Eucalyptus globulus* Labill. decoction extract inhibits the growth of NCI-H460 cells by increasing the p53 levels and altering the cell cycle profile. *Food Funct.* **2019**, *10*, 3188−3197.

(63) Mota, I. S.; Rodrigues Pinto, P. C.; Novo, C.; Sousa, G.; Guerreiro, O.; Guerra, A. N. R.; Duarte, M. F.; Rodrigues, A. E. Extraction of polyphenolic compounds from *Eucalyptus globulus* bark: process optimization and screening for biological activity. *Ind. Eng. Chem. Res.* **2012**, *51*, 6991−7000.